Progress in ECE diagnostics development on TCV

V.S. Udintsev, I. Klimanov, P. Blanchard, H. Weisen, L. Porte, S. Coda, T.P. Goodman, O. Sauter, G.P. Turri, S. Alberti, B.P. Duval, E. Fable, D. Fasel, A. Fasoli, A. Gudozhnik, M.A. Henderson, J.-Ph. Hogge, Ph. Marmillod, K.R. Mason, A. Mueck, R. Patterson, R.A. Pitts, A. Pochelon, Ch. Schlatter, and the TCV Team

Association Euratom-Confédération Suisse, EPFL/SB/CRPP, Station 13, CH-1015 Lausanne, Switzerland

Abstract. ECE diagnostics are powerful tools for studying MHD, heat transport and fast electron dynamics on the Tokamak à Configuration Variable (TCV; R/a = 0.88 m/ 0.24 m, h = 1.5 m, B_T < 1.54 T). The second harmonic X-mode ECE is received from both the Low Field Side (LFS) and the High Field Side (HFS) by separate radiometers to ensure the full radial coverage of the plasma cross-section with a high sampling rate. Because the plasma can be placed at a variety of vertical locations (Z), two lines-of-sight perpendicular to the magnetic field (at Z = 0 cm and Z = +21 cm) are being routinely used by both radiometers to measure the electron radiation temperature. In this paper, some recent scientific results, as well as ECE diagnostics under development, are discussed.

Email of V.S. Udintsev: victor.udintsev@epfl.ch

INTRODUCTION

Electron Cyclotron Emission (ECE) diagnostics on TCV allow to study the electron temperature evolution in time with a good spatial and temporal resolution. ECE diagnostics are widely used to obtain both qualitative and quantitative information on heat transport, magnetohydrodynamic (MHD) phenomena and fast electron dynamics. Recently, oscillations of the electron temperature have been observed on TCV by means of ECE and Soft X-Ray tomography. These oscillations are reminiscent of the oscillations of the central electron temperature (O-regime) seen in low loop voltage or fully non-inductive LHCD plasmas with reversed central magnetic shear on Tore Supra[1]. During the decay of the oscillation, a transition from a 16 kHz to a 7 kHz MHD mode is observed. It is thought that the evolution of the electron temperature, the MHD modes and the current density profile are closely linked to each other, similar to what has been proposed to explain Tore Supra results.

This paper is organized as follows. First, a brief description of the hardware is given. Then, some recent experimental results are discussed. Finally, conclusions and upgrade plans are presented.

ECE DIAGNOSTICS ON TCV

TCV is equipped with two heterodyne radiometers, one viewing from the HFS and the second one from the LFS of the machine perpendicular to the magnetic field. Both are operating in the second harmonic X-mode with the single-side band receiver scheme. The HFS radiometer[2] has 24 channels and covers the frequency range of 78 – 114 GHz. The spatial resolution of the system is about 1 cm and the sampling rate is up to 80 kHz. The LFS radiometer[3] monitors the plasma by 24 channels at 65 – 99 GHz. Because of a large variety of plasma configurations in TCV, each radiometer can be remotely connected to one of several existing lines of sight. The HFS radiometer utilizes two lines of sight at Z = 0 cm and Z = +21.2 cm with respect to the equatorial midplane, whilst the LFS system can be connected via a remotely controlled switch to Z = 0 cm and Z = +21.2 cm lines of sight and to the steerable receiver identical to the TCV X2 ECH launcher[4]. The poloidal sections are different for HFS and LFS radiometer antennas. In this paper, the focus is emphasized on the lines of sight perpendicular to the magnetic field.

For both lines of sight of the HFS radiometer and Z = +21 cm line of the LFS radiometer, a combination of a Gaussian horn and a mirror has been used as antennas. The Gaussian beam waists ($1/e^2$ diameter on the intensity) in the plasma center for these lines of sight are 8 – 10 cm, meaning that the amplitude of any structures in the plasma with poloidal wavenumbers $k_\theta > 0.4$ cm^{-1} will be attenuated[5]. Therefore, it has been decided to install a new TPX (poly 4-methyl-1-pentene) lens antenna at Z = 0 cm for the LFS radiometer. It has a focusing length of 20 cm (instead of 30 cm one used before January 2006) and has been placed just 30 cm away from the one inch circular waveguide, thus allowing to decrease the beam diameter down to $d_\theta = 2.2$ cm at r/a = 0.9 and $d_\theta = 5.5$ cm in the plasma center. This makes the diagnostic more suitable for temperature fluctuation studies by the cross-correlation method[5]. The advantage of having smaller poloidal beam waist for an observation of MHD modes is demonstrated in the next sections. The intermediate frequency (IF) bandwidth of the LFS radiometer B_{IF} is 750 MHz and a video bandwidth for each individual channel B_V is 100 kHz. This defines the radial resolution for each channel to be about 0.5 - 1 cm. The relativistic broadening starts to be important and contributes to the spatial resolution for temperatures above several keVs. The sampling rate varies from 10 kHz to 200 kHz. According to the radiometer equation[6], the minimum detectable temperature[7] (under the assumption that the bandwidth of the temperature source is larger than B_V) is estimated to be 1.6%. This is roughly in agreement with measurements performed during the absolute calibration of the diagnostic. The plasma temperature on TCV varies from 100 eV to 10 keV, so one would expect up to 45 – 50 μW to be collected by an antenna. In order to protect the system from excessive ECH power, two notch filters at 82.7 GHz and 118 GHz are implemented into the radio frequency (RF) part of both radiometers. The loss measurements in the waveguides of the LFS radiometer for the Z = 0 cm line of sight (without the lens, the vacuum window and the switch) are performed by means of calibrated Gunn oscillator and Schottky diode detector and yielded about -7.5 dB. The losses in the third line of sight that includes the steerable receiver for oblique ECE measurement are found to be in order of -15.5 dB. These values may vary slightly for different frequencies. The losses

in the Z = +21 cm line of sight were not yet absolutely measured, however, they are expected to be somewhat larger than for the Z = 0 cm case.

Both HFS transmission lines are similar to the Z = +21 cm line of the LFS radiometer. A detailed description of RF and IF stages, as well as the acquisition systems of both radiometers, has been given in the literature[2-3] and, therefore, is not repeated here. The sketch of the presently constructing correlation ECE diagnostic is given in the last section. The absolute calibration by means of a hot/cold source of both radiometers is not a trivial task on TCV. Because of the room temperature change during the year, calibration factors may change. In the future, the absolute calibration will be performed by means of the calibrated microwave noise source in the frequency range 60 – 118 GHz. Right now, the cross-calibration versus Thomson scattering is being performed on a shot-to-shot basis. It has been found that the calibration factors do not vary much (< 5%) upon changing between various lines of sight by means of the microwave switch in the LFS radiometer transmission line.

RECENT SCIENTIFIC RESULTS FROM ECE ON TCV

ECE is being extensively used in many experimental missions on TCV. In this paper, we report about two kinds of experiments that yielded some interesting results from last campaigns.

Fast electron studies in low-density plasmas

Observation of non-thermal electrons in tokamak plasmas is useful for studies of the confinement of collisionless electrons and aids in understanding of anomalous transport. On TCV, a unique ability of ECE systems to observe simultaneously the plasma from the HFS and the LFS is used to study the fast electrons both qualitatively and quantitatively[2-3]. In order to retrieve qualitative information on fast electrons energy and location, a 3-D NOTEC code to calculate ECE spectra in the tokamak plasma has been utilized[8]. Non-thermal features of ECE spectra are modelled in NOTEC with drifting Maxwellians, temperature anisotropy, loss- and anti-loss cones. A preliminary analysis of the shot #32035 ($T_e(0)$ = 5 keV, $T_e^{rad}(0)$ = 20 keV (from LFS ECE), $n_e(0) = 1.3 \times 10^{19}$ m^{-3}, B_T = 1.45 T, co-ECCD 2 x 500 kW on-axis, 1 x 500 kW ECH at r/a = 0.4) has been done, taking the actual antenna pattern into account. It appears to be that the observed LFS ECE results are in agreement with simulations if one introduces the non-thermal electron population with $T_e^{n\text{-}th}$ = 45 keV and the electron density $n_e^{n\text{-}th} = 0.06 n_e(0)$. These fast electron population exists at r/a = 0 – 0.4. More dedicated simulations of ECE spectra in presence of fast electrons will be done in future.

Temperature oscillations and MHD in the presence of ITB

Very recently, oscillations of the electron temperature have been observed on TCV in low-density on-axis counter-ECCD and off-axis co-ECCD discharges by means of ECE and soft X-ray (SXR) diagnostics[9]. These oscillations have low frequency (8 – 12 Hz), do not have a helical structure (m = 0, n = 0) and, therefore, cannot be ascribed to

the MHD. Two scenarios have been established in which these oscillations occurred. For the first scenario, the plasma is shifted up to Z = +23 cm above the equatorial midplane. After an eITB is established at r/a = 0.4 – 0.5, co-ECCD off-axis is applied at the same location (2 x 500 kW), and the plasma current is driven fully non-inductively. In the second scenario, the plasma is placed at Z = 0 cm and the counter-ECCD is added on-axis, in addition to the Ohmic current. In both cases, oscillations of electron temperature, the total plasma current, the electron density and the plasma core position have been observed. In the first scenario, the oscillations of the plasma current are purely due to the temperature oscillations, as the bootstrap current fraction changes by 40 – 60% (depending on the particular shot conditions) during the oscillation cycle, as calculated by the code LIUQE[10]. However, these discharges are quite difficult for interpretation, as the ECR deposition radius changes upon the plasma core movement by 2 – 4 cm. In the second scenario, the plasma column oscillations are smaller (< 1 cm), and the deposition radius is well inside the barrier. In these plasmas, the loop voltage feedback on the plasma current has been enacted.

In both cases, a strong MHD activity has been detected when the temperature oscillation reaches its maximum. The mode amplitude grows during the whole temperature decay phase from 0.5 cm to 2 cm and decreases during the rise. From fast Mirnov coils, the mode could be identified as 3/1 or 2/1, depending on particular shot. Interestingly, the frequency of the mode drops from 16 kHz down to 6 kHz during the decay of a temperature oscillation (Fig. 1). The diamagnetic frequency, as follows from Thomson scattering measurements, changes by 10 – 20 kHz, if top and the bottom of the oscillation are compared. Because the toroidal and poloidal plasma rotations do not alter much, the possibility that the diamagnetic frequency is the major contributor to the MHD frequency cannot be excluded. However, one should take into account the island size width varies during the oscillation cycle. A detailed analysis of the island width evolution, as well as the mode nature, will be reported elsewhere[11].

Despite the influence of non-thermal electrons on ECE spectra, a precise mode radial location in the shot #32035 has been identified at r/a = 0.4 after high-pass filtering of calibrated LFS ECE signals. The mode localization is in a good agreement with measurements performed for this shot by means of the far-infrared (FIR) diagnostic. Interestingly, the mode is hardly visible by Z = +21 cm line of sight, whilst it is nicely observable by an antenna at Z = 0 cm. In both cases, the island width is roughly the same. The explanation is that the TPX antenna allows to detect structures with k_θ up to 1 cm^{-1} with almost no amplitude attenuation, at the same time as the Z = +21 cm line of sight has high attenuation for $k_\theta < 0.4$ cm^{-1}.

Observations of electron temperature oscillations and associated MHD activity are reminiscent to a so-called O-regime on Tore Supra in fully non-inductively LHCD/ECCD driven plasmas. It has been proposed in Ref.[1] that the O-regime is a regime of an intermediate confinement in which the temperature, the current density profile and the MHD activity are linked to each other. Indeed, in TCV experiments, the H-factor varies from the top to the bottom of the oscillation, being close to the values of those during the sustained eITB on the top. More details will be given elsewhere[11].

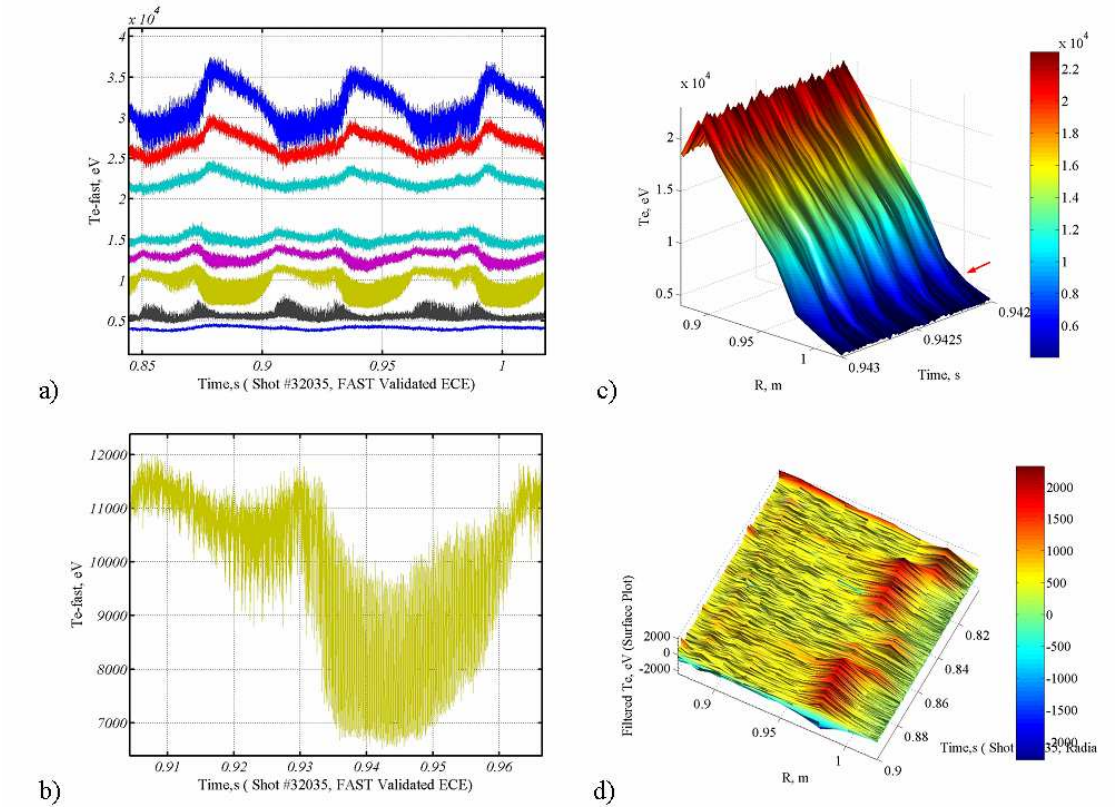

FIGURE 1. (a-b) Evolution of the MHD mode during the cycle of the temperature oscillation in shot #32035; (c) a contour plot of the LFS ECE radiation temperature (the radial position of the mode is indicated by a red arrow); (d) high-pass filtered (at 2 kHz) LFS ECE temperature gives the precise location of the mode at R = 0.98 m (r/a = 0.41) and its evolution during the oscillation cycle.

CONCLUSION AND FUTURE PLANS

In this paper, an ability of TCV ECE diagnostics to obtain some information on fast electron dynamics and to observe MHD modes with a good spatial and temporal resolution has been demonstrated. In the future, studies of the turbulence will be added to the TCV scientific programme. For this purpose, the microwave reflectometer and the correlation ECE branch are currently under development. In this paper, a sketch of the correlation ECE diagnostics is given. Another project that will be implemented on TCV is the vertical ECE system. This diagnostic will provide direct information on the electron energy distribution with very few underlying assumptions. A detailed description of the concept and the hardware will be given in future publications.

Correlation ECE on TCV

Studies of the plasma turbulence are useful for understanding the nature of the transport properties in fusion plasmas. Measurements of electron temperature fluctuations by means of correlation ECE diagnostics have yielded some interesting information on micro-turbulence properties both of electrostatic and magnetic origins on many fusion machines[1,5-7,12-13]. The principles of correlation ECE are described elsewhere[5-7,12-13] and are not repeated here. The scheme in which two sample volumes

are separate in frequency space but overlap in physical space to allow the thermal noise decorrelation as long as the fluctuation correlation length is longer than the sample volume spacing is implemented on TCV (Fig. 2). The experimental setup is very close to this of Tore Supra correlation ECE[5,7]. After the RF part of the LFS radiometer, the correlation ECE is incorporated as a separate IF block, thus allow simultaneous measurements of temperature profiles and fluctuations. In the RF part, a 12 dB amplifier is introduced to compensate for losses caused by the implementation of the correlation ECE. On each of two IF branches, an IF frequency tunable (6 – 18 GHz) YIG filter with 100 MHz bandwidth (at – 3 dB) and integrated 12 bit digital driver is introduced. This allows to monitor the plasma from the plasma center to r/a = 0.6 for the central magnetic field of 1.445 T. Then, the signal is detected by unbiased Schottky diode detectors and amplified by a video amplifier with the variable bandwidth (200 kHz – 500 kHz). Finally, the signal is splitted into two (to separate AC and DC+AC signals) and digitized by a 14-bit acquisition card with a sampling rate up to 3 MHz. The system will allow to observe the temperature fluctuations with an amplitude smaller than a few percent. First results will be presented in a separate paper.

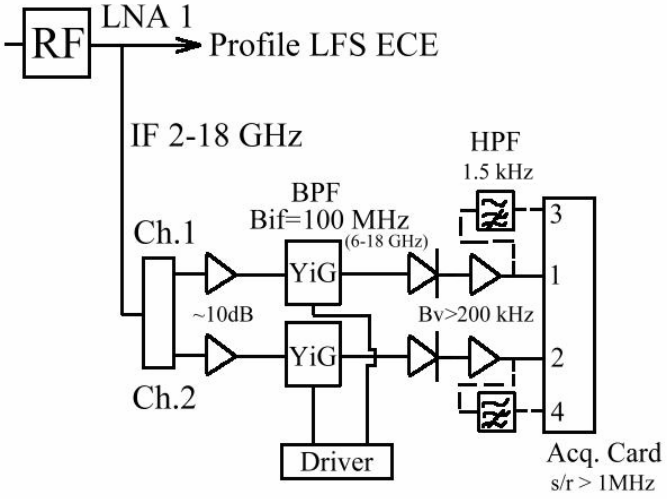

FIGURE 2. A sketch of the future correlation ECE diagnostic on TCV

REFERENCES

1. G. Giruzzi, Plasma Phys. Control. Fusion **47**, B93 (2005).
2. P. Blanchard *et al*., Plasma Phys. Control. Fusion **44**, 2231 (2002).
3. I. Klimanov *et al*., Rev. Sci. Instrum. **76**, 093504 (2005).
4. T.P. Goodman *et al*., this workshop (2006).
5. V.S. Udintsev *et al*., "*First Results of Correlation ECE on Tore Supra*", Fusion Sci. Techn. accepted (2006).
6. H.J. Hartfuss *et al*., Plasma Phys. Control. Fusion **39**, 1693 (1997).
7. V.S. Udintsev *et al*., Plasma Phys. Control. Fusion **48**, L33 (2006).
8. R.M.J. Sillen, Rijnhuizen Report 86-165 (1986); see also V.S. Udintsev *et al*., Rev. Sci. Instrum. **72**, 359 (2001).
9. T.P. Goodman *et al*., Plasma Phys. Control. Fusion **47**, B107 (2005).
10. F. Hoffman and G. Tonetti, Nucl. Fusion **28**, 519 (1988).
11. V.S. Udintsev *et al*., in Proc. of the 33rd EPS Conf., Rome, Italy, D1.003 (2006).
12. S. Sattler and H.J. Hartfuss, Plasma Phys. Control. Fusion **35**, 1285 (1993).
13. G. Cima *et al*., Phys. Plasmas **2**, 720 (1995).